Journal of Organometallic Chemistry 769 (2014) 64–71

Contents lists available at ScienceDirect

Journal of Organometallic Chemistry

journal homepage: www.elsevier.com/locate/jorganchem

Synthesis, X-ray diffraction analysis and nonlinear optical properties of hexacoordinated organotin compounds derived from Schiff bases

Blanca M. Muñoz-Flores [a], Rosa Santillán [b, *], Norberto Farfán [c, *], Violeta Álvarez-Venicio [c], Víctor M. Jiménez-Pérez [a], Mario Rodríguez [d], Omar G. Morales-Saavedra [e], Pascal G. Lacroix [f], Christine Lepetit [f, g], Keitaro Nakatani [h]

[a] Universidad Autónoma de Nuevo León, Facultad de Ciencias Químicas, Av. Universidad S/N, Ciudad Universitaria, San Nicolás de Los Garza Nuevo León, C. P. 66451, México
[b] Departamento de Química, Centro de Investigación y de Estudios Avanzados del IPN, 07000, Apdo. Postal. 14-740, México D. F., Mexico
[c] Facultad de Química, Departamento de Química Orgánica, Universidad Nacional Autónoma de México, Ciudad Universitaria, 04510 México D. F., Mexico
[d] Centro de Investigaciones en Óptica A.P. 1-948, 37000 León, Gto., México
[e] Centro de Ciencias Aplicadas y Desarrollo Tecnológico, Universidad Nacional Autónoma de México, CCADET-UNAM. Circuito Exterior S/N, Ciudad Universitaria AP 70-186, C.P. 04510 México D.F., México
[f] Laboratoire de Chimie de Coordination du CNRS, 205 route de Narbonne, F-31077 Toulouse Cedex 4, France
[g] Université de Toulouse, UPS, INPT, F-31077 Toulouse Cedex 4, France
[h] Laboratoire de Photophysique et Photochimie Supramoléculaires et Macromoléculaires (UMR 8531 du CNRS), Institut d'Alembert Ecole Normale Supérieure de Cachan, Avenue du Président Wilson, 94235 Cachan, France

ARTICLE INFO

Article history:
Received 13 March 2014
Received in revised form
30 June 2014
Accepted 8 July 2014
Available online 17 July 2014

Keywords:
NLO
EFISH
^{119}Sn-NMR
X-ray
Tin compounds

ABSTRACT

The reaction of *N*,*N*-bis(2-hydroxy-4-R-benzylidene)-1,2-phenylendiimine (**1** R = OH, **2** R = OMe) with R'_2SnO (R′ = Me, *n*-Bu, Ph) provided six new organotin derivatives: dimethyl-di-*n*-butyl- and diphenyl [*N*,*N*′-bis(3-hydroxysalicylaldehyde)-1,2-phenylenediiminato]tin(IV) (**1a**), (**1b**), (**1c**) as well as dimethyl-di-*n*-butyl- and diphenyl[*N*,*N*′-bis(3-methoxysalicylaldehyde)-1,2-phenylenediiminato]tin(IV), (**2a**), (**2b**), (**2c**), respectively. All compounds were characterized by ^{1}H, ^{13}C and ^{119}Sn-NMR, elemental analysis, UV, IR, and mass spectrometry. Compounds **2a**, **2b** and **2c** were characterized by single-crystal X-ray structure analysis. In the solid state, **2a**, **2b**, and **2c** showed the Schiff bases backbone in a bent arrangement containing a tin atom with distorted octahedral geometry, where the ligand occupies the four equatorial positions and the methyl, n-butyl, or phenyl groups occupy the *trans* axial positions. The second-order nonlinear optical response of representative organotin compounds **2a**–**c** was estimated by electric field induced second harmonic (EFISH) measurements where interesting β_μ values in the promising range of 10–60 × 10^{-30} esu were evaluated.

Introduction

More than one hundred and sixty years after their discovery by Frankland [1], organotin derivatives are still one of the most investigated areas in organometallic chemistry. As is well-known, organotin complexes have a wide range of applications, in biology, as anti-inflammatory and anti-microbial agents [2], in industry as homogeneous catalysts [3], and in organic chemistry as well [4]. In the last decade there has been considerable interest in the synthesis and characterization of organotin derivatives for application in materials chemistry where gelation [5], anticorrosion [6], CO_2 fixation [7], luminescent [8], and nonlinear optical (NLO) [9] properties have been reported. Metal-organic compounds which show NLO properties play a very important role in the chemistry of materials due to the potential applications in telecommunications, image processing, as optical switches, optic processing of data and generation of new frequencies [10], whereby organic compounds have been the most widely investigated. Organometallic materials which possess structures with electron-donor and electron-withdrawing groups bonded to a planar-π system, have gained considerable attention for nonlinear optics due to their versatility and diversity, *e.g.*, variation in metallic atoms, different oxidation states, neutral and anionic complexes, geometrical environment, variation of ligands, etc. Moreover, the

* Corresponding author. Tel.: +52 55 50 61 37 25; fax: +52 55 50 61 33 89.
E-mail addresses: rsantill@cinvestav.mx (R. Santillán), norberto.farfan@gmail.com (N. Farfán).

http://dx.doi.org/10.1016/j.jorganchem.2014.07.002
0022-328X/

metallic atoms may act as strong donor or acceptor groups being that, one of the basic requirements for NLO response. Also, organometallic complexes should be promising candidates as second-order NLO materials by virtue of their low energy electronic charge transfer excitations. Despite all these advantages, organometallic complexes derived from the main group elements have received less attention.

Our group has reported a series of "*push–pull*" boron complexes (Fig. 1) whereby the possibility of switching NLO properties taking advantage of the rotation of the phenyl ring attached to the boron atom was studied using a semiempirical approach [11]. However, the organic skeleton responsible for NLO properties in the boron derivatives has a bent geometry, leading to chromophores with reduced NLO response. In order to overcome this difficulty, and to extend the range of metal organic NLO materials, we reported the syntheses of four "*push–pull*" diorganotin derivatives [12]. This work showed that this kind of "*push–pull*" diorganotin complexes can be easily prepared, and have better NLO properties than the boron derivatives. The increase of the quadratic hyperpolarizability (β) value is in the order of 1.5 times from the boronate to the tin complexes, which can be attributed to a better planarity of the π-conjugated "push–pull" skeleton responsible for the NLO behavior, as was established by X-ray diffraction studies.

Chiral organotin complexes have also been reported by our group and their nonlinear optical properties were measured showing second harmonic generation (SHG) efficiencies equal to 11 times that of urea in the solid state (Fig. 2) [13]. Other organotin Schiff base complexes exhibit sizeable second harmonic generation (SHG) efficiencies which can be up to 8 times that of urea in the solid state [14]. In turn, the coordination chemistry of mostly bidentate Schiff bases with organotin compounds has received increased attention because they show biological [15] and antitumor activities [16].

In continuation of our research, we designed a series of symmetric organotin complexes from tetradentate Schiff bases with –OH and –OMe donors groups, in order to investigate their NLO responses. The complexes **1a**–**c** and **2a**–**c** are stable and were obtained in high yields (*vide infra*) (Scheme 1).

Results and discussion

Synthesis

The synthesis of the Schiff bases (**1** and **2**) was attained by heating the corresponding 2-hydroxysalicylaldehyde derivative with 1, 2-phenylenediamine in ethanol for 48 h under reflux. The synthesis of compound **2** was previously reported in the literature [17]. The reaction of the appropriate Schiff base and R_2SnCl_2 (R_1 = Me, Bu, or Ph) in triethylamine afforded the corresponding organotin compounds (**1a**–**c** and **2a**–**c**) (Scheme 1). The tin complexes were obtained in good yields.

Spectroscopy data

Selected ^{1}H, ^{119}Sn and ^{13}C NMR data for all compounds are summarized in Table 1. The absence of the OH proton signals bonded to C-2, (13.4 and 13.7 ppm for **1** and **2**) in the complexes evidenced binding of the tin atom to oxygen through the replacement of the phenolic protons. In the ^{1}H NMR spectra of **1a**–**c** and **2a**–**c**, the singlet signals between 8.04 and 8.79 ppm correspond to the imine proton (H-7) and are slightly displaced compared with those of the ligands (8.74 and 8.54 ppm in **1** and **2** respectively).

The ^{119}Sn NMR spectra for **1a**–**c** and **2a**–**c**, show signals in the –384 to –539 ppm range, which is characteristic for this type of hexacoordinated tin derivatives containing N→Sn coordination bonds [18]. For complexes **1c** and **2c**, which have phenyl substituents linked directly to the tin atom, the ^{119}Sn chemical shift signals appear at –530.8 and –539.1 ppm, respectively, while **1a**, **1b**, **2a** and **2b**, which possess methyl and *n*-butyl substituent, show values in the range between –384.4 and –425.2 ppm, consistent with the data reported in the literature [19].

The ^{13}C NMR spectra of tin compounds **1a**–**c** and **2a**–**c** show the imine signal between 161.2 and 163.0 ppm, similar to the corresponding ligands (163.7 and 162.5). In turn C-2 is shifted to higher frequency in the complexes, 172.4–174.2 ppm for **1a**–**c** and **2a**–**c** compared to the ligands (164.2 and 164.7 for **1** and **2** respectively), this is indicative that the phenolic hydrogen has been replaced by the tin atom. The infrared spectra of ligands **1** and **2** (Table 1) show the imine bands at 1609 and 1612 cm^{-1}, while the same band appears between 1600 and 1610 cm^{-1} in **1a**–**c** and **2a**–**c**, due to the Sn–N coordination. Mass spectra show the molecular ion in low abundance for all compounds, and the presence of the tin atom is easily detected from the isotopic pattern of tin [20].

Molecular structure

The details of the crystal data and summary of the collection parameters for **2a**, **2b** and **2c** are given in Table 2; selected bond lengths and angles are summarized in Table 3. X-ray diffraction studies of **2a**, **2b** and **2c** (Figs. 3–5, respectively) corroborate that all molecules contain a hexacoordinated tin atom and a bent ligand skeleton; where both organic moieties are in *trans* position and nitrogens and oxygens in equatorial disposition. The N→Sn distances are in the range of 2.229(3)–2.273(3) Å, in agreement with the values observed in similar organotin compounds derivate from tetradentate Schiff bases [21] [organotin compounds with butyl 2.266(2) and 2.279(19) Å and phenyl 2.22(2) and 2.20(2) Å]. Based on the bond angles, the metallic atoms reside in a distorted octahedral geometry. The two C–Sn distances in **2c** are 2.147(3) and 2.133(3) Å and are thus shorter compared to similar hexacoordinated tin compound (C–Sn 2.18(3) Å) reported in the literature [21]. A water molecule is present in the asymmetric unit cell; which shows a dimeric arrangement in compound **2a** through hydrogen bonds. Compound **2c** also shows a dimeric arrangement due to

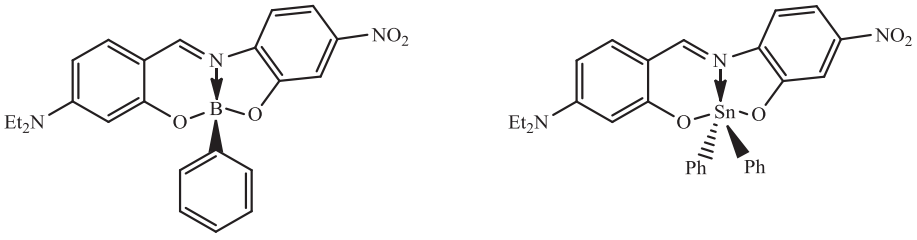

Fig. 1. Boron and tin derivatives of Schiff bases.

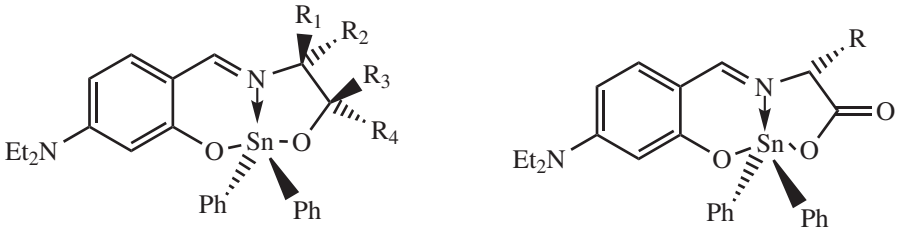

R_1 = Me, H
R_2 = H, Ph
R_3 = H. Me, Ph
R_4 = H, Ph

R = H, Me,tBu, nBu, CH_2OH, Ph, Bz

Fig. 2. Coordinated organotin compounds.

hydrogen bond interactions with the methanol molecule present in the unit cell.

NLO properties

EFISH experimental results

According to the NLO/EFISH-technique [22] the centrosymmetry of an isotropic organic dissolution comprising dipolar molecules can be broken by applying strong DC electric fields to the sample. This leads to a homogeneous dipolar alignment of the organic compounds and to measurable SHG-signals. The resulting quadratic susceptibility in EFISH experiments can be expressed in terms of $\chi^{(2)} \cong NF\gamma E^0$, where N represents the number of molecules per unit volume, F the local field factor and γ the overall EFISH hyperpolarizability given by $\gamma = \gamma_e + (\mu \cdot \beta)/5kT$. Here γ_e represents the cubic electronic contribution and $\mu \cdot \beta/5kT$ the quadratic orientational part, being μ the ground state dipole moment of the studied chromophores and β the vector component of the hyperpolarizability tensor β_{ijk} along the dipole moment direction. In 1D *push–pull* compounds β and μ are parallel which implies a straightforward theoretical analysis (assuming the Kleinman symmetry). The $\mu \cdot \beta$ scalar dot product can then be inferred from a careful analysis of the Maker Fringe experimental data, taking into account the amplitude-period oscillations details. Accordingly, the NLO/EFISH response of complexes **2a**–**c** were measured in chloroform phases (see Table 4) where $\mu \cdot \beta$ values in the interesting range of $10–60 \times 10^{-30}$ have been estimated. It can be seen from Table 4 that the incorporation of different functional R_1 substituents (with R = OMe fixed in this case) affects the magnitude of the $\mu \cdot \beta$ physical parameter in a ratio > 3, being the largest $\mu \cdot \beta$ value found for the $Sn(Ph)_2$ complex followed by the $Sn(Bu)_2$ and $Sn(Me)_2$ ones, respectively. This implies improved intramolecular charge transfer properties between the donor groups and the central acceptor imine moieties for the $Sn(Ph)_2$ complex. The obtained values are however in the same order of magnitude. We argue, based on our experimental results and on the projected 3D molecular geometries, that the symmetrical monomeric bent shape of these compounds and the nearly asymmetric "out-of-plane" position of the R_1 (Me, Bu, Ph) functional groups (considering for instance a mirror-image symmetry), forming hexacoordinated $Sn(Me)_2$, $Sn(Bu)_2$ and $Sn(Ph)_2$ complexes, basically determine the electronic and NLO-performance of the organotin derivatives, delivering comparable NLO capabilities. Indeed, the overall non-planar molecular structure of these compounds is expected to deeply influence the delocalization of electron density over the whole molecular architecture, giving rise to multi-dimensional charge transfer systems and to complex hyperpolarizability β_{ijk} tensors within triclinic space group symmetries. However, for the current family of organotin derivatives under EFISH dipolar testing, the dominant pseudo-one-dimensional and vectorial character of the quadratic NLO-response results in similar charge transfer processes occurring from the alkyl and aryl fragments through the tin-coordinated system. However, there is an effect of the $Sn(R_1)_2$ moieties for the enhancement/variations of the quadratic NLO properties of these compounds probably due to differences between the Sn–N and Sn–C distances. According to Table 3 and the molecular architecture of the **2a**–**c** complexes, the most asymmetric moiety is the $Sn(Me)_2$/(**2a**) followed by the $Sn(Bu)_2$/(**2b**) and

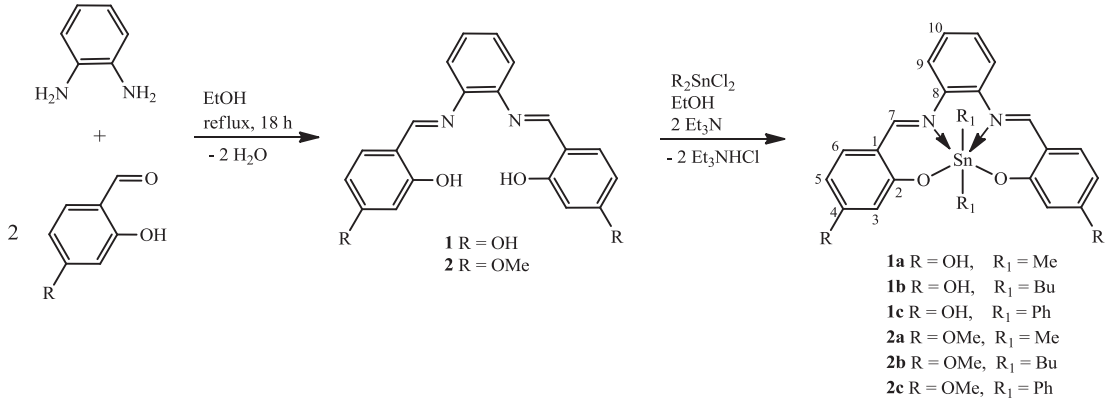

Scheme 1. Synthesis of the Schiff bases and hexacoordinated tin compounds.

Table 1
Selected ^{1}H, ^{119}Sn and ^{13}C (ppm) and stretching vibrations of the C=N bonds (cm^{-1}).

Comp.	^{1}H	^{13}C				^{119}Sn	IR (C=N)
	H-7	C-2	C-4	C-7	C-9		
1	8.74	164.2	163.4	163.7	127.9		1609
2	8.54	164.7	164.5	162.5	127.6		1612
1a	8.54	172.8	166.5	163.0	127.8	−405.4	1602
1b	8.56	173.6	166.8	163.0	128.9	−425.2	1600
1c	8.79	172.4	167.0	162.7	128.3	−539.1	1600
2a	8.23	173.5	167.7	161.7	127.5	−384.4	1601
2b	8.04	174.2	168.0	161.9	127.8	−408.8	1610
2c	8.35	173.2	167.6	161.2	127.9	−530.8	1609

the $Sn(Ph)_2$/(**2c**), respectively. In this way, due to the lack of strong and symmetrical $Sn(R_1)_2$ donor/acceptor groups, the EFISH/NLO-properties of compounds **2a**–**c** are mainly governed by the overall molecular tendency to form polar structures from non-centrosymmetric triclinic space groups, from the stationary contribution of the R = OMe functional group (similar to the R = OH group) strongly conjugated to the imine groups and from the characteristic dipolar moment of the organotin derivatives; thus producing $\mu\cdot\beta$ values in the same order of magnitude. Besides, according to theoretical results [9b], dipolar "*push–pull*" compounds exhibiting similar UV–vis absorbance spectra (as it is the case for the **2a**–**c** complexes) should likely possess β values lying in the same order of magnitude. As the overall molecular structure and electronic/optical properties of the **2a**–**c** complexes are grossly preserved within the corresponding $Sn(R_1)_2$ substitutions, the expected NLO/EFISH modulations should likely arise from geometric rather than $Sn(R_1)_2$ electronic modifications. Therefore the incorporation of asymmetric (in length) or fully symmetric (mirror-image symmetry from the molecular "plane") $Sn(R_1)_2$ moieties could dramatically enhance or modify the NLO-performance of these kinds of complexes. The obtained $\mu\cdot\beta$ values are, in any case, in good agreement compared with analogous nickel derivatives [23].

Theoretical studies

Theoretical insights for the understanding of the substituent effects on the NLO response of the present complexes have been targeted by density functional theory (DFT) computations. A set of three compounds (**1b**, **2b**, and **2c**) was selected to rationalize the effect of the ancillary R_1 ligand on the tin atom, and to evaluate the relative effect of R (OH, OMe) on the overall NLO responses of the complexes. The computed NLO data are gathered in Table 4, in which β is the vectorial component of the hyperpolarizability (see experimental section) and $\mu \times \beta$ is the product of the dipole moment by the β projection along the dipole moment direction. At first glance, it appears that the computed NLO response ($\mu \times \beta$) is far reduced versus that determined experimentally. Apart from the possibility of NLO enhancement frequently observed experimentally with respect to the computed static value (at $\lambda = \infty$), it has to be pointed out that the most relevant computed data has to be found in the tendency observed for a set of substituents to modify significantly the resulting NLO response within a series of related molecules, such as the present tin derivatives.

Along this line, the first thing to observe is that β is very weakly influenced by the nature of the substituents. It has long been known that, in molecular materials, the NLO effects arise from intramolecular charge transfers between electron rich and deficient substituents linked by π-conjugated bridges [24]. It is therefore not surprising that two substituents of similar donating capabilities (OH and OMe) conjugated to the same imine moieties lead to complexes of similar β (**1b** vs **2b**). Similarly, no significant charge transfer is anticipated from the alkyl and aryl fragments through the tin atom, leading to $Sn(Bu)_2$ and $Sn(Ph)_2$ complexes of similar β (**2b** vs **2c**). Finally, the main differences in the **1b**, **2b** and **2c** series would likely arise from dipole moments. The relative orientation of μ and β is a key parameter in the evaluation of the magnitude of the $\mu \times \beta$ value. In most "*push–pull*" NLO molecules, the computed μ value is large (e.g. 10 D) and parallel to β, which greatly simplify the understanding of the origin of the NLO response ($\mu \times \beta$). In the present case, and due to a lack of strong donor/acceptor character, μ is far reduced and falls in the 1–2 D range. Moreover, its orientation with respect to β appears to strongly depend on small chemical and conformational changes difficult to fully rationalize. All together these computational insights lead to the idea that, if the β values are almost the same in these materials, the experimental EFISH values would likely reflect various dipolar effects, considering the fact that the μ magnitude will be modest in any cases.

Table 2
Crystal data for **2a**, **2b** and **2c**.

Data	**2a**	**2b**	**2c**
Chemical formula	$C_{24}H_{24}N_2O_4Sn\cdot H_2O$	$C_{30}H_{36}N_2O_4Sn\cdot H_2O$	$C_{34}H_{28}N_2O_4Sn\cdot CH_3OH$
Formula weight	523.16	607.17	648.11
Crystal system	Triclinic	Triclinic	Triclinic
Space group	P-1	P-1	P-1
a, [Å]	10.4741(2)	11.245 (2)	9.3181 (3)
b, [Å]	11.0024(2)	11.451 (2)	10.1147(3)
c, [Å]	11.0098(2)	11.813 (2)	17.24584(4)
α, [°]	82.7690(10)	96.223 (7)	87.247(2)
β, [°]	76.1870(10)	99.189 (7)	87.305(2)
γ, [°]	68.9470(10)	99.579 (8)	74.2590(10)
V, [$Å^3$]	1148.71(4)	1466.0 (4)	1561.68(8)
Z	2	2	2
Temp, [K]	293(2)	293(2)	293(2)
Refl. collected	24,411	13,664	8606
Refl. unique	5465	4632	5841
Refl. observed (4σ)	13,642	5994	7710
Goodness	1.048	1.067	1.061
No. variables	305	403	371
Final R (4σ)	0.0323	0.0289	0.0481
Final wR_2	0.0732	0.0688	0.1253

Conclusions

We have reported five new hexacoordinated tin compounds; the similarities in spectra of all compounds studied here and the X-ray crystal structures for compounds **2a**, **2b** and **2c** confirm hexacoordinated tin atoms with a distorted octahedral geometry.

Compounds **2a**–**b** exhibit reasonably good quadratic NLO properties where $\mu\cdot\beta$ values comparable to similar nickel-based compounds have been found. In these studies, differences in the experimental and theoretical $\mu\cdot\beta$ NLO parameter larger than 300% have been determined according to the EFISH technique for the $Sn(R_1)_2$ complexes. Such differences are more likely to arise from the projection of β along the dipole moment (changes in the $\mu\beta$ relative angles, considering similar β values for the **2a**–**c** complexes) than from the $Sn(R_1)_2$ substitution.

Experimental section

Instruments

All starting materials were commercially available. Solvents were used without further purification. Melting points were recorded on an Electrothermal 9200 apparatus and are uncorrected. Infrared spectra were measured on a FT-IR Perkin–Elmer Spectrum GSX spectrophotometer using KBr pellets. ^{1}H, ^{13}C and

Table 3
Selected bond lengths (Å) and angles (°) for **2a**, **2b**, and **2c**.

	Lengths (Å)				Angles (°)		
	2a	**2b**	**2c**		**2a**	**2b**	**2c**
C(7)–N(1)	1.300(3)	1.304(4)	1.295(5)	C–Sn–C	166.12(11)	163.53(11)	167.15(14)
C(14)–N(2)	1.303(3)	1.294(4)	1.313(5)	O–Sn–O	125.26(7)	127.10(7)	125.29(10)
Sn(1)–O(2)	2.1975(17)	2.2139(18)	2.214(2)	N–Sn–N	72.64(7)	72.62(8)	72.83(11)
Sn(1)–O(3)	2.2187(18)	2.2212(17)	2.165(2)				
Sn(1)–N(1)	2.261 (2)	2.269(2)	2.250(3)				
Sn(1)–N(2)	2.252(2)	2.273(3)	2.229(3)				
Sn(1)–C(23)	2.126(3)	2.149(3)	2.133(3)				
Sn(1)–C(27)	–	2.131(3)	–				
Sn(1)–C(29)	–	–	2.147(3)				
Sn(1)–C(24)	2.126(3)	–	–				

^{119}Sn-NMR spectra were recorded on a Bruker advance DPX-300, Jeol GSX 270 and Jeol Eclipse +400 spectrometers. Chemical shifts (ppm) are relative to $(CH_3)_4Si$ for ^{1}H and ^{13}C and $Sn(CH_3)_4$ for ^{119}Sn. Mass spectra were recorded on a Hewlett Packard 5989A spectrometer. Elemental analyses were carried out on a Thermo Finnigan Flash EA 1112 elemental microanalyzer.

X-ray data collection and structure determination

In all cases the single crystals suitable for X-ray structural studies were obtained by slow evaporation from a solution of each compound in mixtures of $CHCl_3$ and hexane. The crystal data were recorded on an Enraf Nonius Kappa-CCD (λ MoKα = 0.71073 Å, graphite monochromator, T = 293 K-CCD rotating images scan mode). The crystals were mounted on a Lindeman tube. Absorption corrections were performed using the SHELX-A program [25]. All reflection data set were corrected for Lorentz and polarization effects. The first structure solution was obtained using the SHELXS-97 program and then SHELXL-97 program was applied for refinement and output data [19]. All software manipulations were done under the WIN-GX environment program set [26]. Molecular perspectives were drawn under ORTEP3 drawing application [27]. All heavier atoms were found by Fourier map difference and refined anisotropically. Some hydrogen atoms were found by Fourier map differences and refined isotropically. The remaining hydrogen atoms were geometrically modeled and are not refined.

NLO/EFISH measurements

The second-harmonic generation (SHG) activity and the experimental evaluation of the molecular hyperpolarizabilities (β) of the studied compounds were performed according to the electric field induced second harmonic (EFISH) technique [28]. In the current case, chloroform-based solutions (at ~6.8×10^{-4} M) of compounds **2a**–**c** were prepared for EFISH measurements. A nanosecond-pulsed Q-switched Nd:YAG laser system (at 10 Hz) was implemented as the fundamental excitation beam (λ_ω = 1.064 μm) inducing the representative SHG Maker-fringe patterns in the organic liquid samples. The Maker-fringe amplitude oscillations were obtained by translating a home-made wedge-shaped glass cell (BK7 glass blades fixed around $\theta = 4°$) orthogonally to the laser beam direction. The glass cells were placed between two flat large-area stainless steel electrodes connected to a high voltage supply (at 5.7 kV) synchronized with the available laser source. The generated SHG-signals ($\lambda_{2\omega} = 0.532$ μm) were conveniently filtered and detected by a photomultiplier tube connected to a digital oscilloscope. Both a urea power sample and a pure chloroform solution were used for reference and calibration purposes.

Computational details

The quadratic molecular hyperpolarizabilities (β) of the tin derivatives were investigated computationally, at the B3PW91/6-31G**/LANL2DZ(Sn) level [29], using the finite field (FF) procedure available in the Gaussian09 package [30]. B3PW91 was selected as the functional for the computations in relation to its

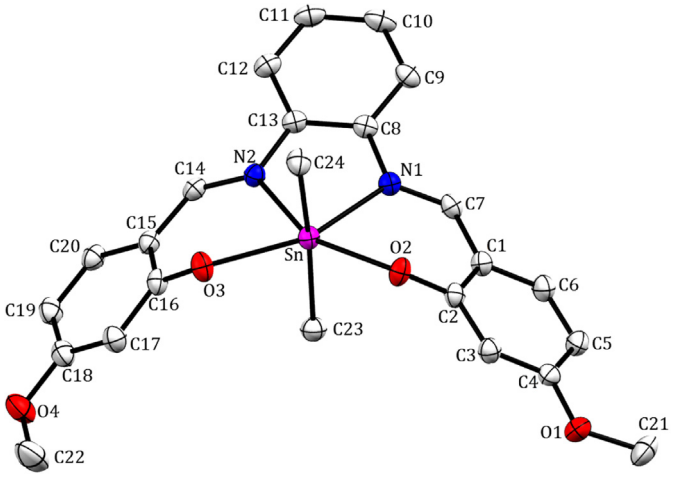

Fig. 3. Crystal structure of compound **2a**. Hydrogens were omitted for clarity.

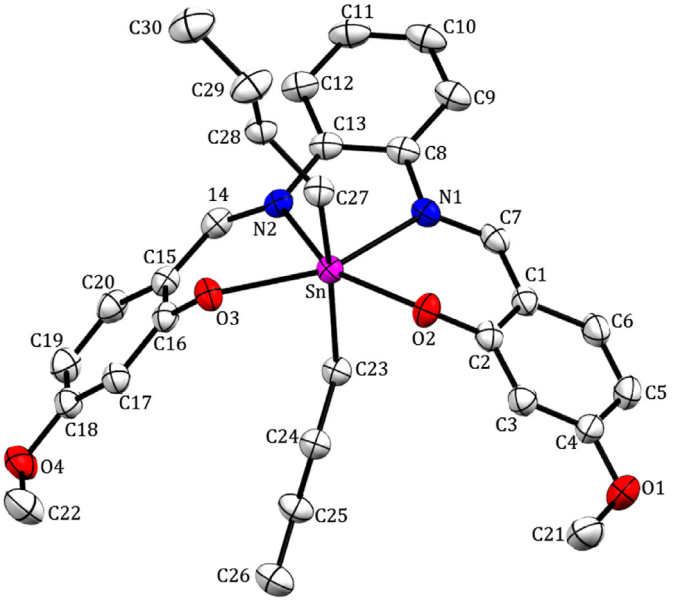

Fig. 4. Crystal structure of compound **2b**. Hydrogens were omitted for clarity.

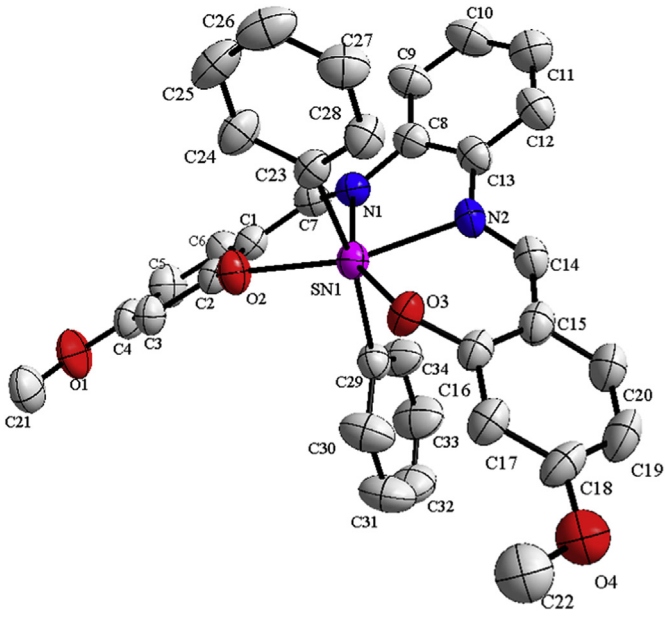

Fig. 5. Crystal structure of compound **2c**. Hydrogens were omitted for clarity.

previous use in related tin derivatives [12–14], the LANL2DZ pseudo-potential being used to account for relativistic effects on the tin atom. The molecular structures were first fully optimized without any symmetry constraints. Vibrational analysis was performed at the same level in order to check the obtention of a minimum on the potential energy surfaces.

The calculations of the hyperpolarizabilities were performed with the default value of Field strength of 0.001 atomic units. In the FF approach, β is obtained as the numerical partial derivative of the energy (W) with respect to the electric field (E), evaluated at zero field according to the following equation:

$$\beta_{ijk} = -\left(\frac{\partial^3 W}{\partial E_i \partial E_j \partial E_k}\right)_{E=0} \quad (3)$$

an expression which is only valid for the static field limit. Following this approach, β is the magnitude of the vectorial hyperpolarizability ($\beta = \sqrt{(\beta_x)^2 + (\beta_y)^2 + (\beta_z)^2}$ with $\beta_i = \beta_{ixx} + \beta_{iyy} + \beta_{izz}$, after assumption of the Kleinman symmetry conditions [31].

Syntheses

Ligands **1** [32] and **2** [33] were synthesized by reacting salicylaldehyde, or 4-methoxysalicylaldehyde with 2-phenylenediimine in a 2:1 ratio, in ethanol under reflux.

Table 4
DFT Computed and experimental NLO data for Representative Tin Schiff-base Complexes.

Compounds	β (cal)	μ (cal)	$\mu \times \beta$ (cal)	$\mu\cdot\beta$ (exp) (1064 nm)	Angle: $\mu\beta$ (deg.)
1b	19.0	2.07	25.7		49.3
2a		1.23		14.8	
2b	19.0	1.35	12.0	48.2	117.9
2c	19.9	1.64	13.2	56.4	66.2

β in 10^{-30} cm^5 esu^{-1} and μ in Debye.

The following procedure was used in the syntheses of compounds **1a**-**1c** and **2a**–**c**, the ligands **1**, **2** and the corresponding tin compounds were stirred in ethanol for 12–24 h with triethylamine. The precipitate was filtrated under vacuum and washed with hexane, followed by recrystallization from chloroform-hexane solution.

*N,N-Bis(2,4-dihydroxybenzylidene)-1,2-phenylenediimine (**1**)*

Compound **1** was obtained from 2.76 g (20 mmol) of 2, 4-dihydroxybenzaldehyde and 1.08 g (10 mmol) of 1,2-phenylenediimine. The product was obtained as a yellow solid (3.10 g), yield 89%, mp 224 °C. IR (KBr) ν_{max} (cm^{-1}): 3179 (OH), 3174 (OH), 2898, 2518, 1609 (C=N), 1574, 1545, 1500, 1356, 1307, 1231, 1209, 1181, 1153, 1122, 979, 845, 743, 697, 531. MS m/z (%): 349 (M^++1, 12), 348 (M^+, 43), 228 (26), 227 (55), 226 (100), 212 (21), 119 (21); ^{1}H NMR (300 MHz, DMSO-d_6) δ (ppm): 6.29 (1H, d, J = 2.2 Hz, H-3), 6.39 (1H, dd, J = 2.2, 8.5 Hz, H-5), 7.31 (1H, dd, J = 7.5, 1.5 Hz, H-9) 7.37 (1H, dd, J = 7.5, 1.5 Hz, H-10), 7.43 (1H, d, J = 8.5 Hz, H-6), 8.74 (1H, s, H-7), 10.40 (1H, s, OH), 13.42 (1H, s, OH); ^{13}C NMR (75.4 MHz, DMSO-d_6) δ (ppm): 103.2 (C-3), 108.7 (C-5), 113.1 (C-1), 120.3 (C-10), 127.9 (C-9), 135.3 (C-6), 142.8 (C-8), 163.4, 164.2 (C-4, C-2), 163.7 (C-7). HRMS calc. m/z for $C_{20}H_{16}N_2O_4$ [M^++H]$^+$: 349.1183; Found 349.1183.

*Dimethyl[N,N′-bis(3-hydroxysalicylaldehyde)-1,2-phenylenediiminato]tin(IV) (**1a**)*

Compound **1a** was obtained from the reaction of 0.348 g (1 mmol) of compound **1** and 0.22 g (1 mmol) of dichlorodimethyltin. The product was obtained as a yellow solid (0.368 g), yield 74%, m.p. >350 °C. IR (KBr) ν_{max} (cm^{-1}): 3350 (OH), 2909, 2597, 1602 (C=N), 1527, 1494, 1440, 1358, 1238, 1179, 1126, 978, 890, 844, 796, 756, 668. MS m/z (%): 497 (M^++1, 4), 476 (M^+, 5), 481 (98), 466 (14), 348 (17), 329 (14), 226 (100), 212 (16), 165 (25), 132 (27); ^{1}H NMR (300 MHz, DMSO-d_6) δ (ppm): 0.39 [3H, s, ^2J (^{119}Sn–^{1}H) = 104.6 Hz, CH_3], 5.92 (1H, d, J = 2.0 Hz, H-3), 6.09 (1H, dd, J = 2.0, 8.8 Hz, H-5), 7.25 (1H, d, J = 8.8 Hz, H-6), 7.29 (1H, dd, J = 7.5, 1.5 Hz, H-9), 7.38 (1H, dd, J = 7.5, 1.5 Hz, H-10), 8.54 [1H, s, ^3J (^{119}Sn–^{1}H) = 129.02 Hz, H-7], 10.18 (1H, s, OH); ^{13}C NMR (75.4 MHz, DMSO-d_6) δ (ppm): 7.4 [^1J (^{119}Sn–^{13}C) = 1081.2 Hz, ^1J (^{117}Sn–^{13}C) = 1036.2 Hz, CH_3], 106.5 (C-3), 106.9 (C-5), 114.5 (C-1), 118.6 (C-10), 127.8 (C-9), 139.6 (C-6), 140.0 (C-8), 163.0 (C-7), 166.5 (C-4), 172.8 (C-2); ^{119}Sn-NMR (149.08 MHz, DMSO-d_6) δ (ppm): −405.4. HRMS calc. m/z for $C_{22}H_{20}N_2O_4Sn$ [M^++H]$^+$: 497.0522; Found 497.0521.

*Di-n-butyl[N,N′-bis(3-hydroxysalicylaldehyde)-1,2-phenylenediiminato]tin(IV) (**1b**)*

Compound **1b** was obtained from 0.348 g (1.00 mmol) of compound **1** and 0.304 g (1 mmol) of dichlorodibutyltin. The product was obtained as a yellow solid (0.476 g), yield 82%, m.p. 203 °C. IR (KBr) ν_{max} (cm^{-1}): 3246 (OH), 3071, 2953, 2922, 2858, 2608, 1600 (C=N), 1575, 1545, 1487, 1439, 1381, 1235, 1185, 1126, 976, 849, 796, 752, 663, 622, 485. MS m/z (%): 581 (M^++1, 1), 580 (M^+, 1), 523 (34), 330 (12), 269 (9), 226 (100), 169 (28), 110 (17), 43 (22); ^{1}H NMR (300 MHz, DMSO-d_6) δ (ppm): 0.59 (3H, t, J = 9.7 Hz, H-14), 1.02–1.15 (4H, m, H-13, H-12), 1.29–1.31 (2H, m, H-11), 5.91 (1H, d, J = 2.1 Hz, H-3), 6.09 (1H, dd, J = 2.1, 8.8 Hz, H-5), 7.24 (1H, d, J = 8.8 Hz, H-6), 7.29 (1H, dd, J = 7.5, 1.5 Hz, H-9), 7.51 (1H, dd, J = 7.5, 1.5 Hz, H-10), 8.56 (1H, s, H-7), 10.14 (OH); ^{13}C NMR (75.4 MHz, DMSO-d_6) δ (ppm): 14.3(C-14), 26.6 (C-12), 26.7 (C-13), 28.3 (C-11), 106.8 (C-3), 107.1 (C-5), 114.9 (C-1), 118.6 (C-10), 128.8 (C-9), 140.0 (C-6), 140.7 (C-8), 163.0 (C-7), 166.8 (C-4), 173.6 (C-2); ^{119}Sn-NMR (149.08 MHz, DMSO-d_6) δ (ppm): −425.2. HRMS calc. m/z for $C_{28}H_{32}N_2O_4Sn$ [M^++H]$^+$: 581.1463; Found 581.1463.

*Diphenyl[N,N′-bis(3-hydroxysalicylaldehyde)-1,2-phenylenediiminato]tin(IV) (**1c**)*

Compound **1c** was obtained from 0.348 g (1 mmol) of compound **1** and 0.344 g (1 mmol) of dichlorodiphenyltin. The product was obtained as a yellow solid (0.47 g), yield 76%, m.p. 213 °C. IR (KBr) ν_{max} (cm^{-1}): 3183 (OH), 2983, 2788, 2721, 1600 (C=N), 1594, 1575, 1541, 1475, 1435, 1390, 1221, 1178, 1125, 986, 852, 775, 736, 697. MS *m/z* (%): 621 (M^++1, 40), 620 (M^+, 20), 619 (35), 543 (100), 541 (75), 307 (88), 289 (51), 255 (71), 242 (98), 219 (20) 165 (15); ^{1}H NMR (300 MHz, DMSO-d_6) δ (ppm): 5.94 (1H, d, J = 1.9 Hz, H-3), 6.07 (1H, dd, J = 1.9, 8.8 Hz, H-5), 7.08–7.13 (3H, m, H-*m*, H-*p*), 7.23 (1H, d, J = 8.8 Hz, H-6), 7.29 (1H, dd, J = 7.5, 1.5 Hz, H-9), 7.57 (1H, dd, J = 7.5, 1.5 Hz, H-10), 7.45 (1H, m, H-*o*), 8.79 (1H, s, H-7), 10.59 (1H, s, OH); ^{13}C NMR (75.4 MHz, DMSO-d_6) δ (ppm): 107.3 (C-3), 107.7 (C-5), 114.6 (C-1), 118.4 (C-10), 128.1 [^4J (^{119}Sn–^{13}C) = 47.4 Hz, C-*p*], 128.2 [^3J(^{119}Sn–^{13}C) = 108.8 Hz, C-*m*), 128.3 (C-9), 135.4 [^2J(^{119}Sn–^{13}C) = 60.5 Hz, C-*o*), 138.9 (C-6), 140.5 (C-8), 150.5 (C-*i*), 162.7 (C-7), 167.0 (C-4), 172.4 (C-2); ^{119}Sn-NMR (149.08 MHz, DMSO-d_6) δ (ppm): −539.1. HRMS calc. *m/z* for $C_{32}H_{24}N_2O_4Sn$ $[M^+ + H]^+$: 621.0837; Found 621.0840.

*N,N-Bis(2-hydroxy-4-methoxybenzylidene)-1,2-phenylenediimine (**2**)*

Compound **2** was obtained from 3.04 g (20 mmol) of 4-methoxysalicylaldehyde and 1.08 g (10 mmol) of 1,2-phenylenediimine. The product was obtained as a yellow solid (2.85 g), yield 76%, m.p. 176 °C. IR (KBr) ν_{max} (cm^{-1}): 3275 (OH), 3059, 3012, 2968, 2839, 1612 (C=N), 1585, 1568, 1512, 1464, 1439, 1371, 1341, 1293, 1244, 1203, 1169, 1136, 1115, 1032, 967, 888, 829, 747, 649. MS *m/z* (%): 377(M^++1, 17), 376 (M^+, 64), 240 (100), 226 (17), 197 (2), 137 (6); ^{1}H NMR (300 MHz, DMSO-d_6) δ (ppm): 3.83 (3H, s, OMe), 6.48 (1H, dd, J = 2.4, 8.6 Hz, H-5), 6.56 (1H, d, J = 2.4 Hz, H-3), 7.22 (1H, dd, J = 7.5, 1.5 Hz, H-9), 7.28 (1H, dd, J = 7.5, 1.5 Hz, H-10), 7.27 (1H, d, J = 8.6 Hz, H-6), 8.54 (1H, s, H-7), 13.65 (1H, s, OH); ^{13}C NMR (75.4 MHz, DMSO-d_6) δ (ppm): 55.86 (OMe), 101.6 (C-3), 107.6 (C-5), 113.6 (C-1), 119.8 (C-10), 127.6 (C-9), 133.9 (C-6), 142.6 (C-8), 162.5 (C-7), 164.5164.7 (C-4, C-2); Elemental analysis calc. for $C_{22}H_{20}O_4N_2$: C 70.27, H 5.32, and N 7.45%. Found: C 70.05, H 5.89, and N 7.31%.

*Dimethyl[N,N′-bis(3-methoxysalicylaldehyde)-1,2-phenylenediiminato]tin(IV) (**2a**)*

Compound **2a** was obtained from 0.376 g (1 mmol) of compound **2** and 0.219 g (1 mmol) of dichlorodimethyltin. The product was obtained as a yellow solid (0.49 g), yield 94%, m.p. 245 °C. IR (KBr) ν_{max} (cm^{-1}): 3006, 2931, 2833, 1601 (C=N), 1575, 1519, 1419, 1391, 1358, 1305, 1257, 1204, 1182, 1143, 1123, 1027, 974, 836, 791, 753, 616. MS *m/z* (%): 525 (M^++1, 1), 524 (M^+, 2), 513 (17), 510 (25), 509 (100), 508 (43), 507 (74), 506 (33), 505 (41), 358 (8), 343 (13); ^{1}H NMR (300 MHz, DMSO-d_6) δ (ppm): 0.69 [3H, s, ^2J(^{119}Sn–^{1}H) = 105.4 Hz, ^2J(^{117}Sn–^{1}H) = 100.9 Hz, CH_3), 3.79 (3H, s, OMe), 6.17 (1H, d, J = 2.4 Hz, H-3), 6.21 (1H, dd, J = 2.4, 8.9 Hz, H-5), 7.05 (1H, d, J = 8.9 Hz, H-6), 7.29 (1H, dd, J = 7.5, 1.5 Hz, H-9), 7.34 (1H, dd, J = 7.5, 1.5 Hz, H-10), 8.23 [1H, s, ^3J (^{119}Sn–^{1}H) = 12.86 Hz, H-7]; ^{13}C NMR (75.4 MHz, DMSO-d_6) δ (ppm): 6.24 [^1J(^{119}Sn–^{13}C) = 4099.1 Hz, ^1J(^{117}Sn–^{13}C) = 3913.4 Hz, CH_3), 55.33 (OMe), 103.9 (C-3), 107.2 (C-5), 114.3 (C-1), 117.7 (C-10), 127.5 (C-9), 137.4 (C-6), 140.4 (C-8), 161.7 (C-7), 167.7 (C-4), 173.5 (C-2); ^{119}Sn-NMR (111.88 MHz, DMSO-d_6) δ (ppm): −384.4. HRMS calc. *m/z* for $C_{24}H_{24}N_2O_4Sn$ $[M^+ + H]^+$: 525.0836; Found 525.0832.

*Di-n-butyl[N,N′-bis(3-methoxysalicylaldehyde)-1,2-phenylenediiminato]tin(IV) (**2b**)*

Compound **2b** was obtained from 0.376 g (1 mmol) of compound **2** and 0.304 g (1 mmol) of dichlorodibutyltin. The product was obtained as a yellow solid (0.496 g), yield 82%, m.p. = 202 °C. IR (KBr) ν_{max} (cm^{-1}): 3445, 2926, 2861, 2346, 1610 (C=N), 1574, 1514, 1381, 1314, 1209, 1122, 1026, 974, 838, 750, 616, 521. MS *m/z* (%): 607 (M^++1, 0.5), 608 (M^+, 0.2), 555 (16.6), 552 (28.6), 551 (100), 494 (18), 370 (11.4), 358 (12.7), 240 (4.8), 192 (4), 163 (6.8); ^{1}H NMR (270 MHz, $CDCl_3$) δ (ppm): 0.63 (3H, t, J = 7.2 Hz, H-14), 1.09–1.21 (4H, m, H-13, H-12), 1.39–1.57 (2H, m, H-11), 3.78 (OMe), 6.17–6.19 (2H, m, H-3, H-5), 7.04 (1H, d, J = 9.4 Hz, H-6), 7.26–7.29 (2H, m, H-9, H-10), 8.24 (1H, s, H-7); ^{13}C NMR (75.47 MHz, $CDCl_3$) δ (ppm): 14.1 (C-14), 25.6, 26.8 (C-12, C-13), 28.5 (C-11), 55.8 (OMe), 104.4 (C-3), 107.4 (C-5), 114.9 (C-1), 117.9 (C-10), 127.8 (C-9), 137.9 (C-6), 141.3 (C-8), 161.9 (C-7), 168.0 (C-4), 174.4 (C-2); ^{119}Sn-NMR (100.74 MHz, $CDCl_3$) δ (ppm): −408.8. HRMS calc. *m/z* for $C_{30}H_{36}N_2O_4Sn$ $[M^+ + H]^+$: 609.1776; Found 609.1773.

*Diphenyl[N,N′-bis(3-methoxysalicylaldehyde)-1,2-phenylenediiminato]tin(IV) (**2c**)*

Compound **2c** was obtained from 0.376 g (1 mmol) of compound **2** and 0.344 g (1 mmol) of dichlorodiphenyltin. The product was obtained as a yellow solid (0.52 g), yield 80%, m.p. 229 °C. IR (KBr) ν_{max} (cm^{-1}): 3063, 2938, 1609 (C=N), 1573, 1515, 1460, 1440, 1420, 1383, 1312, 1236, 1211, 1187, 1126, 1021, 975, 843, 795, 736, 697, 661, 618. MS *m/z* (%): 649 (M^++1, 1), 648 (M^+, 2), 572 (33), 571 (100), 570 (49), 569 (79), 567 (44), 255 (6); ^{1}H NMR (400 MHz, $CDCl_3$) δ (ppm): 3.73 (3H, s, OMe), 6.11 (1H, dd, J = 2.4, 8.8 Hz, H-5), 6.16 (1H, d, J = 2.4 Hz, H-3), 6.95 (1H, d, J = 8.8 Hz, H-6), 7.09–7.12 (3H, m, H-*m*, H-*p*), 7.27 (1H, dd, J = 7.5, 1.5 Hz, H-9), 7.33 (1H, dd, J = 7.5, 1.5 Hz, H-10), 7.62 (2H, dd, J = 1.7, 7.7 Hz, H-*o*), 8.35 (1H, s, H-7); ^{13}C NMR (100 MHz, $CDCl_3$) δ (ppm): 55.4 (OMe), 104.8 (C-3), 107.4 (C-5), 114.4 (C-1), 117.3 (C-10), 127.5 [^{4}J(^{119}Sn–^{13}C) = 148.6 Hz, C-*p*], 127.6 [^{3}J(^{119}Sn–^{13}C) = 450.0 Hz, C-*m*], 127.9 (C-9), 135.2 [^{2}J(^{19}Sn–^{13}C) = 247.7 Hz, C-*o*), 137.7 (C-6), 139.4 (C-8), 147.3 (C-*i*), 161.2 (C-7), 167.6 (C-4), 173.2 (C-2); ^{119}Sn-NMR (120.48 MHz, DMSO-d_6) δ (ppm): −530.8. Elemental analysis calc. for $C_{34}H_{28}O_4N_2Sn{-}H_2O$: C 61.38, H 4.54, and N 4.21%. Found: C 61.32, H 4.99, and N 4.04%.

Appendix A. Supplementary material

CCDC 1009493, 990674 and 990675 contain the supplementary crystallographic data for this paper. These data can be obtained free of charge from The Cambridge Crystallographic Data Centre via www.ccdc.cam.ac.uk/data_request/cif.

Acknowledgments

Financial support from CONACyT, UNAM (PAPIIT IN-214513), UNAM-DGAPA and ECOS program (ECOS action #M11PP01) is acknowledged. Thanks are given to Marco A. Leyva for X-ray data collection. The theoretical studies were performed using HPC resources from CALMIP (Grant 2013 [0851]]).

References

[1] (a) E. Frankland, Liebigs Ann. Chem. 71 (1849) 171;
(b) E. Frankland, J. Chem. Soc. 2 (1850) 267.
[2] M. Nath, S. Pokharia, G. Eng, X. Song, A. Kumar, Eur. J. Med. Chem. 40 (2005) 289.
[3] K. Orita, Y. Sakamoto, K. Hamada, A. Mitsutome, J. Otera, Tetrahedron 55 (1999) 2899.
[4] (a) M. Kosugi, K. Fugami, J. Organomet. Chem. 653 (2002) 50;
(b) T. Bruce Grindley, Tin in Organic Synthesis, in: M. Gielen, et al. (Eds.), Tin Chemistry Fundamentals, Frontiers, and Applications, John Wiley & Sons, Ltd, 2008.
[5] V. Chandrasekhar, K. Gopal, P. Singh, R.S. Narayanan, A. Dithie, Organometallics 28 (2009) 4593.

[6] H.I. Beltrán, R. Esquivel, A. Sosa-Sánchez, J.L. Sosa-Sánchez, H. Höpfl, V. Barba, N. Farfán, M. Galicia García, O. Olivares-Xometl, L.S. Zamudio-Rivera, Inorg. Chem. 43 (2004) 3555.
[7] (a) B. Mairychová, L. Dostál, A. Růžička, L. Beneš, R. Jambor, J. Organomet. Chem. 699 (2012) 1;
(b) J. Beckmann, D. Dakternieks, A. Duthie, N.A. Lewcenko, C. Mitchell, Angew. Chem. Int. Ed. 43 (2004) 6683.
[8] (a) M.C. García-López, B.M. Muñoz-Flores, V.M. Jiménez-Pérez, I. Moggio, E. Arias, R. Chan-Navarro, R. Santillán, Dyes Pigm. 106 (2014) 188;
(b) W.-Q. Geng, H.-P. Zhou, L.-H. Cheng, F.-Y. Hao, G.-Y. Xu, F.-X. Zhou, Z.-P. Yu, Z. Zheng, J.-Q. Wang, J.-Y. Wu, Y.-P. Tian, Polyhedron 31 (2012) 738;
(c) S.M. Crawford, A.A.-S. Ali, T.S. Cameron, A. Thompson, Inorg. Chem. 50 (2011) 8207;
(d) X.-J. Zhao, Q.-F. Zhang, D.-C. Li, J.-M. Dou, D.-Q. Wang, J. Organomet. Chem. 695 (2010) 2134;
(e) E. López-Torres, A.L. Medina-Castillo, J.F. Fernández-Sánchez, M.A. Mendiola, J. Organomet. Chem. 695 (2010) 2305;
(f) S.-L. Cai, Y. Chen, W.-X. Sun, H. Li, Y. Chen, S.-S. Yuan, Bioorg. Med. Chem. Lett. 20 (2010) 5649.
[9] (a) D.G. Li, R.T. Hu, W. Zhou, P.P. Sun, Y.H. Kan, Y.P. Tian, H.P. Zhou, J.Y. Wu, X.T. Tao, M.H. Jiang, Eur. J. Inorg. Chem. (2009) 2664;
(b) P.G. Lacroix, N. Farfán, Quadratic Nonlinear Optical Properties of Tin-Based Coordination Compounds, in: M. Gielen, et al. (Eds.), Tin Chemistry: Fundamentals, Frontiers and Applications, John Wiley and Sons, 2008, p. 351 (Chapter 3.6);
(c) J.M. Rivera, D. Guzmán, M. Rodríguez, J.F. Lamère, K. Nakatani, R. Santillán, P.G. Lacroix, N. Farfán, J. Organomet. Chem. 691 (2006) 1722;
(d) J.M. Rivera, H. Reyes, A. Cortés, R. Santillán, P.G. Lacroix, C. Lepetit, N. Farfán, Chem. Mater. 18 (2006) 1174.
[10] (a) O. Marget, P.G. Lacroix, J.P. Costes, B. Donnadieu, C. Lepetit, K. Nakatani, Inorg. Chem. 43 (2004) 4743;
(b) F. Averseng, C. Lepetit, P.G. Lacroix, J.P. Tuchagues, Chem. Mater. 12 (2000) 2225;
(c) M. Lequan, C. Branger, J. Simon, T. Thami, E. Chauchard, A. Persoons, Chem. Phys. Lett. 229 (1994) 101;
(d) M. Lequan, C. Branger, J. Simon, T. Thami, E. Chauchard, A. Persoons, Adv. Mater. 6 (1994) 851.
[11] H. Reyes, B.M. Muñoz, N. Farfán, R. Santillán, S. Rojas-Lima, P.G. Lacroix, K. Nakatani, J. Mater. Chem. 12 (2002) 2898.
[12] H. Reyes, C. García, N. Farfán, R. Santillan, P.G. Lacroix, K. Nakatani, C. Lepetit, J. Organomet. Chem. 689 (2004) 2303.
[13] J.M. Rivera, H. Reyes, A. Cortés, R. Santillan, P.G. Lacroix, C. Lepetit, K. Nakatani, N. Farfán, Chem. Mater. 18 (2006) 1174.
[14] J.M. Rivera, D. Guzmán, M. Rodríguez, J.F. Lamère, R. Santillan, P.G. Lacroix, K. Nakatani, N. Farfán, J. Organomet. Chem. 691 (2006) 1722.
[15] M. Nath, R. Yadav, M. Gielen, H. Dalil, D. de Vos, G. Eng, Appl. Organomet. Chem. 11 (1997) 727.
[16] M. Gielen, P. Lelieved, D. de Vos, R. Willem, In Vitro Antitumour Activity of Organotin Compounds, in: M. Gielen (Ed.), Metal-based Antitumour Drugs, vol. 2, Freund, tel Aviv, 1992, p. 29.
[17] D.K. Dey, M.K. Saha, M.K. Das, N. Bhartiya, R.K. Bansal, G. Roasir, S. Mitra, Polyhedron 18 (1999) 2687.
[18] J. Otera, J. Organomet. Chem. 221 (1981) 57. D.K. Dey, M.K. Das, R.K. Bansal, J. Organomet. Chem. 535 (1997) 7.
[19] P.J. Smith, A.P. Tupciauskas, Ann. Rep. NMR Spectrosc. 8 (1978) 291.
[20] M.R. Liszow, T.R. Spalding, Mass Spectroscopy of Inorganic and Organometallic Compounds, Elsevier Scientific Publishing Company, Amsterdam-London-New York, 1973, p. 209.
[21] S.G. Teoh, G.Y. Yeap, C. C Loh, L.W. Foong, S.B. Teo, H.K. Fun, Polyhedron 16 (1997) 2213.
[22] (a) C. Bosshard, G. Knöpfle, P. Prêtre, P. Günter, J. Appl. Phys. 71 (1992) 1594;
(b) I. Maltey, J.A. Delaire, K. Nakatani, P. Wang, X. Shi, S. Wu, Adv. Mater. Opt. Electron. 6 (1996) 233;
(c) C.S. Liu, R. Glaser, P. Sharp, J.F. Kauffmann, J. Phys. Chem. A 101 (1997) 7176.
[23] S. Di Bella, I. Fragala, I. Ledoux, M.A. Diaz-García, T.J. Marks, J. Am. Chem. Soc. 119 (1997) 9550.
[24] D.J. Williams, Angew. Chem. Int. Ed. Eng. 23 (1984) 690–703.
[25] G.M. Sheldrick, SHELX97, Programs for Crystal Structure Solution and Refinement, University of Goettingen, Goettingen, 1997.
[26] L.J. Farrugia, J. Appl. Crystallogr. 32 (1999) 837.
[27] ORTEP 3L L.J. Farrugia, J. Appl. Crystallogr. 30 (1997) 837.
[28] (a) J.L. Oudar, J. Chem. Phys. 67 (1977) 446;
(b) B.F. Levine, C.G. Betha, J. Chem. Phys. 63 (1975) 2666;
(c) B.F. Levine, C.G. Betha, J. Chem. Phys. 65 (1976) 1989;
(d) I. Maltey, J.A. Delaire, K. Nakatani, P. Wang, X. Shi, S. Wu, Adv. Mater. Opt. Electron. 6 (1996) 233.
[29] (a) A.D. Becke, J. Chem. Phys. 98 (1993) 1372;
(b) J.P. Perdew, Y. Wang, Phys. Rev. B 45 (1992) 13244.
[30] M.J. Frisch, G.W. Trucks, H.B. Schlegel, G.E. Scuseria, M.A. Robb, J.R. Cheeseman, G. Scalmani, V. Barone, B. Mennucci, G.A. Petersson, H. Nakatsuji, M. Caricato, X. Li, H.P. Hratchian, A.F. Izmaylov, J. Bloino, G. Zheng, J.L. Sonnenberg, M. Hada, M. Ehara, K. Toyota, R. Fukuda, J. Hasegawa, M. Ishida, T. Nakajima, Y. Honda, O. Kitao, H. Nakai, T. Vreven, J.A. Montgomery Jr., J.E. Peralta, F. Ogliaro, M. Bearpark, J.J. Heyd, E. Brothers, K.N. Kudin, V.N. Staroverov, R. Kobayashi, J. Normand, K. Raghavachari, A. Rendell, J.C. Burant, S.S. Iyengar, J. Tomasi, M. Cossi, N. Rega, J.M. Millam, M. Klene, J.E. Knox, J.B. Cross, V. Bakken, C. Adamo, J. Jaramillo, R. Gomperts, R.E. Stratmann, O. Yazyev, A.J. Austin, R. Cammi, C. Pomelli, J.W. Ochterski, R.L. Martin, K. Morokuma, V.G. Zakrzewski, G.A. Voth, P. Salvador, J.J. Dannenberg, S. Dapprich, A.D. Daniels, Ö. Farkas, J.B. Foresman, J.V. Ortiz, J. Cioslowski, D.J. Fox, Gaussian 09, Revision D.01, Gaussian, Inc., Wallingford CT, 2009.
[31] D.A. Kleinman, Phys. Rev. 126 (1962) 1977.
[32] A. Soroceanu, S. Shova, M. Cazacu, I. Balan, N. Gorinchoy, C. Turta, J. Chem. Crystallogr. 43 (2013) 310.
[33] A. Shokrollahi, M. Ghaedi, S. Alipour, A.H. Kianfar, Eur. J. Chem. 2 (2011) 324.